



Winter 12-2022

Investigations Into PRG-2 and its Involvement in Developing Gallus Gallus Retinal Neurons

Jeffrey Parham

Follow this and additional works at: <https://digitalcommons.winthrop.edu/graduatetheses>



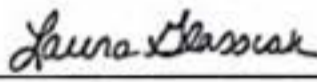
Part of the [Biology Commons](#), [Cell Biology Commons](#), and the [Molecular Biology Commons](#)

To the Dean of the Graduate School:

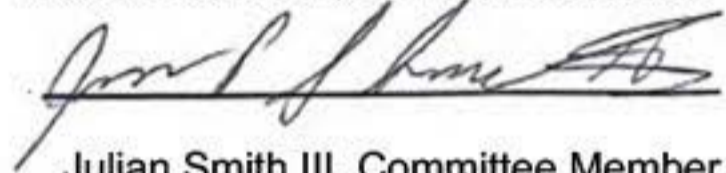
We are submitting a thesis written by Jeffrey Emanuel Parham entitled
Investigations into PRG-2 and its involvement in developing *Gallus gallus* retinal
neurons. We recommend acceptance in partial fulfillment of the requirements for
the Degree of Master of Science



Eric Birgbauer, Thesis Adviser



Laura Glasscock, Committee Member



Julian Smith III, Committee Member



Takita Sumter, Dean,
College of Arts and Science



M. Gregory Oakes,
Acting Dean, Graduate School

INVESTIGATIONS INTO PRG-2 AND ITS INVOLVEMENT IN DEVELOPING *GALLUS*
GALLUS RETINAL NEURONS

A Thesis
Presented to the Faculty
Of the
College of Arts and Sciences
In Partial Fulfillment
Of the
Requirements for the Degree
Of
Master of Science
In Biology
Winthrop University
December, 2022
By
Jeffrey Emanuel Parham

Abstract

I am interested in the development of the nervous system, especially since during development nerves grow and extend, but in adults, they do not regenerate if damaged. We are specifically interested in the molecules that guide nerves to the correct target during their development. Lysophosphatidic acid (LPA) is a bioactive molecule that has been shown to play a role in neural development. LPA, through repeated studies, has been shown to stop neurons from growing by causing a physical change in a neuron's growth cone (a structure used for navigation and growth). Recently, a novel set of genes, called PRGs, have been demonstrated to interact with LPA and LPA receptors. However, interaction between PRGs and LPA is not well understood. Thus, I investigated the role of PRG and LPA in neuronal development, focused on the visual system in chicken embryos. During this study I determined expression of PRG genes in the developing chicken eye using RT-PCR. Then I designed target sequences for mutation of chicken PRG gene using CRISPR and cloned targeting guides. I designed six guide RNAs (gRNAs) to target one specific PRG-2 gene determined by the expression studies. I then evaluated these gRNA constructs to determine if they efficiently mutate PRG-2 in cells. This project then required delivery of my gRNA DNA constructs to embryonic chicken eyes via electroporation to induce mutations in the retinal ganglion cells (RGCs) of the eye that compose the optic nerve which I optimized. I then overexpressed PRG-2/GFP fusion protein in chicken fibroblast cells to confirm my construct would be a candidate for overexpression in chicken retina.

Table of Contents

Abstract.....	ii
List of Tables.....	v
List of Illustrations.....	vi
Chapter 1: Literature Review of PRG.....	1
Neurological Disease, Central Nervous System Injury.....	2
Central Nervous System Development.....	3
Lysophosphatidic Acid Receptor-mediated Signaling.....	5
Plasticity Related Genes.....	6
Chapter 2: Materials and Methods.....	10
Determining PRG-2 Expression.....	11
gRNA Design.....	12
gRNA Isolations.....	13
Cell Culture, Transfection of DF1-Cas9 Cells.....	14
Cell Sorting, DNA Isolation.....	14
PCR-Amplification of Mutation.....	15
Mutation Validation.....	16
<i>Ex ovo</i> Chicken Embryo Culture, Injection, and Electroporation	
Optimization.....	16
Overexpression of GFP-PRG-2 Construct.....	17
Chapter 3: Results.....	18
Expression.....	19
System to Mutate PRG-2 Using CRISPR.....	20
System for Overexpression of PRG-2.....	21
Chapter 4: Discussion.....	27

System for Knockdown Of PRG-2 using CRISPR.....	28
System for Overexpression.....	29
References.....	34

List of Tables

Table 1.....	12
Table 2.....	13
Table 3.....	15
Table 4.....	25

List of Illustrations

Figure 1	4
Figure 2	23
Figure 3	24
Figure 4	24
Figure 5	26
Figure 6	26
Figure 7	31
Figure 8	32
Figure 9	32
Figure 10	33
Figure 11	33

Chapter One

Literature Review of PRG

Neurological Disease, Central Nervous System Injury

The central nervous system (CNS) in vertebrates is a highly organized system composed of millions of cells (Waxenbaum et al. 2021). The CNS is composed of two parts: the brain and the spinal cord. All other neurons extending from the spinal cord to the rest of the body make up the Peripheral Nervous System (PNS). These two systems coordinate all the biochemical interactions that occur in an organism (Waxenbaum et al. 2021). Understanding how these vast numbers of cells differentiate, grow, communicate, and organize, ultimately developing into the nervous system, is a central focus in the foundations of neuroscience. One reason neuroscientists focus on nervous system development is the hope of finding a cure for neuropathological diseases—most neuropathological diseases affecting the CNS result in neurological damage. Depending on the system involved, the damage could be either transient, healing over time, or permanent, resulting in neuronal cell loss.

The PNS of most species exhibits regenerative abilities. When injured or damaged, neuronal cells regenerate and reestablish functionality. Conversely, at least in humans, the CNS does not "naturally" demonstrate this capability (Mietto et al. 2015). Multiple neurodegenerative diseases affect the central nervous system, including Alzheimer's disease (AD), Parkinson's disease (PD), amyotrophic lateral sclerosis (ALS), multiple sclerosis (MS), Huntington's disease, and multiple system atrophy, which all result in lasting damage to the CNS (Mietto et al. 2015). This damage in mammals over time leads to neuronal loss or dysfunction; however, in a wide range of lower animals, this neuronal loss can be restored through a regenerative mechanism. The PNS and CNS, in most species, can correct the damage done by pathological insult (Richardson et al. 1980). However, in most vertebrates like humans, injured neuronal cells in the CNS demonstrate anti-regenerative properties that prevent them from restoring functions and reestablishing connections after injury (Schwab and Caroni 1988). This contrasts

with the PNS neurons, which regenerate when injured, eventually restoring function over time (Huebner and Strittmatter 2009). Understanding how the CNS develops and organizes would explain how these inhibitory qualities are expressed and ways to overcome their inhibition. Ultimately, overcoming the inhibition of nerve regeneration would give neuroscientists a possible therapeutic tool for treating neuropathological diseases affecting the CNS.

Central Nervous System Development

The CNS must develop in a specific way to successfully manage an organism's functions. The developing cells of the CNS extend axons that navigate through the environment by sending and receiving information through chemical stimuli (Figure 1). Axons use a chemo-sensitive structure called a growth cone to respond to extracellular chemical stimuli and navigate to their appropriate targets (Tessier-Lavigne and Goodman 1996). The CNS develops its neuronal circuitry by extending axons through a multitude of tissues. Axons must navigate through dense cellular regions to specific target areas to form this circuitry, including synaptic connections with other neurons. The vast number of cells, axons, and connections make investigating development difficult. Therefore, neuroscientists often use the visual system to model nerve growth in CNS development because of its particular topographical organization and easy accessibility (Erskine and Herrera 2007). In the visual system, retinal ganglion cells (RGCs) in the eye project axons toward the brain in a highly reproducible pattern (Huberman et al. 2003), suggesting axons use guidance cues to find their way in their visual map formation. These guidance cues are all integrated by the growth cone.

The growth cone is composed of an actin network and associated microfilaments at its distal end and at its proximal end, microtubules made of tubulin. Growth cones are located at the end of growing axons and are lined with receptors that allow the cell to

respond to molecular cues in the extracellular environment (Huberman et al. 2003). When activated, the receptors lining the growth cone lead to a cascade of signaling pathways, such as Rho and ROCK, that results in the tubulin and actin polymerizing at the distal tip to generate microtubules and microfilaments respectively (Fincher et al. 2014). Growth cones are activated by axon guidance molecules that promote axonal growth toward a target or repulse axons away from a target. Axon guidance molecules can be localized originating from surrounding or originating from distance sources act over long distances to determine the routes developing axons follow to their targets (Tessier-Lavigne and Goodman 1996). Several known axon guidance molecules include netrins, slits, semaphorins, and ephrins. Recently, lysophosphatidic acid (LPA) has been theorized to be an axon guidance molecule (Birgbauer 2021; Birgbauer and Chun 2010; Fincher et al. 2014)

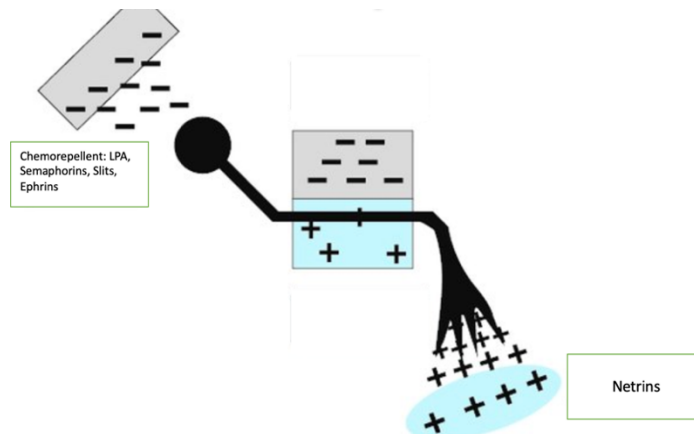


Figure 1: Retinal ganglion cells (Black circle) extend axons (Black Line) through an extracellular environment rich with guidance cues. These guidance cues can be attractive such as Netrins (plus in blue) or repellent such as LPA (minus in grey). The axon uses a special structure called a growth cone (Black projections) to interpret guidance cues. The growth cone guides the axon to its destination in development by responding to the extracellular environment using receptors. Multiple types of guidance cues and receptors have been identified that direct the projections taken during axonal development.

Lysophosphatidic Acid Receptor-mediated Signaling

Lysophosphatidic acid (LPA) is a monoacyl-*sn*-glycerol-3-phosphate bioactive lysophospholipid with a phosphoglycerol head and a single tail (Birgbauer 2021). It belongs to a class of bioactive molecules, each with differing fatty acid chain lengths and degrees of saturation. LPA is expressed by many tissues and is produced by two pathways: hydrolysis of phosphatidic acid (PA) by phospholipase A1 and A2 or cleavage of lysophosphatidylcholine (LPC) by autotaxin. LPA receptors are highly expressed in the brain. LPA has been found to play a role in neural development by inducing growth cone collapse and neurite retraction via a receptor-mediated signaling response (Fukushima et al. 2001). Multiple receptors have been hypothesized to induce this cell signaling, including the family of six G coupled protein receptor (GPCR) LPAR 1-6, which couple with multiple G-proteins ($G_{12/13}$, G_i , G_q , G_s). Although LPARs have been well characterized, their specific effect on axonal growth is poorly understood due to functional redundancy in their pathway activation (Birgbauer 2021). These activated pathways generally result in microfilament and cytoskeletal rearrangements, which provide the motility needed by neurons to navigate to specific targets. Previous research showed that cultured RGC axon growth cones collapse dose-dependently when exposed to LPA (Birgbauer and Chun 2010; Fincher et al. 2014). Incongruously, LPA-receptor knockout mice for some of the LPA receptors did not lead to significant neuronal aberrations or inhibitory growth cone effects in retinal growth cones (Birgbauer and Chun 2010). However, multiple studies have shown that LPA may be involved in axon guidance in the brain and retina (Birgbauer 2021), which may suggest alternative LPA-dependent signaling pathways independent of the classic GPCR. Thus, significant work is still needed to classify LPA as a *bona fide* axon guidance molecule and to identify its corresponding receptors.

LPA is known to be enzymatically inactivated by lipid phosphate phosphatases (LPPs), a superfamily of cell surface protein receptors. LPPs are characterized by six transmembrane domains containing highly conserved enzymatically active domains (Bräuer et al. 2003). Some members of the LPP superfamily, namely, LPP1-3 and splice variant LPP1A, can degrade LPA (Alderton et al. 2001). A novel sub-family of membrane-bound LPPs, plasticity-related genes (PRG1-5), was recently identified while investigating brain plasticity mechanisms. Sequence alignments show homology between PRGs and LPPs, specifically LPP1 (Brauer 2008). Interestingly, PRGs 1-5 are all vertebrate-specific and offer varying expression patterns in brain tissue throughout development. Overexpression of PRG-1 in neuronal cell lines protects developing axons from LPA-induced neurite collapse (Bräuer et al. 2003). Additionally, PRG-1 overexpression increases the LPA degradation product monoacylglycerol (MAG) (Bräuer et al. 2003). LPA is suggested to guide thalamic axons to the cortex of PRG-2 null mice (Cheng et al. 2016). Furthermore, PRGs are linked to axonal growth, neurite shaft protrusion in primary neurons, and dendritic spine formation (Yu et al. 2015). PRG is a subfamily of transmembrane proteins that possibly have different or redundant modes of action with LPA (Bräuer et al. 2003). The interaction between PRGs and LPAs is not well understood.

Plasticity Related Genes

PRG-1 was the first in the family to be discovered while investigating the mechanism by which the hippocampus typically develops and heals after injury in humans (Bräuer et al. 2003). For instance, they found that when hippocampal axons from the entorhinal cortex are transected, the remaining axons demonstrate regenerative axon sprouting into denervated zones. While investigating the molecular mechanisms responsible for this hippocampal plasticity, the protein receptor PRG-1 was found to

have a distinct expression pattern starting at embryonic day 19 (E19). In parallel, axons of the hippocampus grow from the entorhinal cortex at E19 *in vivo*. This expression and parallel growth suggested that PRG-1 played a role in axonal development and regenerative sprouting. Since its discovery, PRG-1 expression has been identified in the cerebellar cortex, olfactory bulb, cerebral cortex, and caudate putamen (Tokumitsu et al. 2010). PRG has been observed in neuronal axons to facilitate lipid phosphate degradation and fiber outgrowth in a repellent environment (Bräuer et al. 2003). Axons (when grown in an LPA-rich environment) of younger E16 mice that lack PRG-1 will undergo neurite retraction; however, older E19 mice axons that express PRG-1 grown in the same environment resist this retraction in a dose-dependent manner. Interestingly, after a lesion occurs in the hippocampus, PRG-1 is upregulated within 24 hours in denervated areas (Bräuer et al. 2003). The behavior of axons with and without PRG-1 expression in the presence of LPA strengthened support for PRG-1's involvement in axonal guidance. In contrast, LPA-specific receptors LPA-1, LPA-2, and LPA-3 are also expressed in developing neurons and could account for the observed neurite retraction seen by Brauer et al. (2003). However, unlike PRG-1, there is no corresponding difference in the expression pattern of LPA-specific receptors throughout E16-E19 development when LPA responses change. The lack of LPA-receptor regulation suggests that the observed attenuation of neurite retraction results from only PRG-1 and no other known LPA-specific receptors. Additionally, others have demonstrated that PRG-1 can interfere with signal transduction through LPA interactions at the synaptic cleft (Trimbuch et al. 2009). Trimbuch et al. (2009) observed that PRG-1 knockout mice had a corresponding 50% reduction in the uptake of fluorescence-labeled LPA. Extracellular LPA signaling is essential for CNS development and postmitotic neurons provide an endogenous source for LPA (Fukushima et al. 2001). Others have shown evidence that PRG-1 reduces available extracellular LPA, thus attenuating repulsive

signaling (Trimbuch et al. 2009). Similarly, others have shown PRG-1 deletion or mutation results in aberrant synaptic signaling within glutamatergic neurons due to altered lipid processing (Liu et al. 2016; Schneider et al. 2018; Vogt et al. 2017). These observations, in total, suggest that PRG-1 plays a pivotal role in response to LPA and might also be responsible for how the axon's growth cone responds to LPA, which typically results in neurite collapse during development. Sequence homology between PRGs suggests other members may play a similar role as PRG-1 during development.

PRG-3 is another member of the LPP subfamily that shows high sequence homology to PRG-1 and 2. PRG-3 is highly regulated during development and is expressed as early as E16. PRG-3 is expressed in the hippocampus, but expression levels are lowered throughout development (Wang and Molnár 2005). Unlike PRG-1, PRG-3 does not have brain-specific expression and is also found in the liver, kidney, and testis (Savaskan et al. 2004). Overexpression of PRG-3 promotes filopodia formation and neurite shaft protrusion, possibly through the ROCK and Rho pathways (Broggini et al. 2016; Velmans et al. 2013). Additionally, PRG-3 shRNA knockdown or knockout experiments have reduced neurite protrusion (Velmans et al. 2013). It has been shown that PRG-3 knockouts lead to morphological changes within neuronal cell lines. Although PRG-3 expressing N1E-115 cells show no LPA ectophosphatase activity (Savaskan et al. 2004), overexpression of PRG-3 in cortical neurons after injury promotes axonal regeneration (Fink et al. 2017). This functionality could be attributed to the C-terminal tail of the PRGs located on the cytoplasmic side of the membrane. The cytoplasmic tail position is suggestive of a regulatory or signal transduction domain. PRG-3 has a short C-terminal tail compared to the long 400aa tail of PRG-1.

PRG-5, the last of the PRG family to be characterized, it has a short C-terminal domain that interacts with various phosphorylated phosphatidylinositols such as the LPA-precursor PA (Coiro et al. 2014). Moreover, PRG-5 has been found to attenuate

LPA-induced neurite retraction in N1E-115 cells (Broggini et al. 2010; Coiro et al. 2014). Thus, PRG-5's observed interactions with phosphorylated lipids suggest that the C-terminal tails on PRGs play a crucial role in their lipid binding and axonal development. Overexpression studies of PRG-5 in neurons reveal filopodia formation and neurite growth (Broggini et al. 2010; Coiro et al. 2014). Equally important, PRG-5 shows differential expression throughout development in the hippocampus and spinal cord (Broggini et al. 2010).

PRG-2, like PRG-1, has a long 400 amino acid C-terminal domain. Additionally, PRG-2 has similar ectophosphatase domains to PRG-1 (Cheng et al. 2016). PRG-2 was shown to be involved with LPA-induced thalamic axonal guidance in mice, where LPA production was reduced by inhibiting autotaxin (an LPA synthesizing enzyme) which resulted in aberrant axonal extensions. *Moreover*, when grown on an LPA-rich substrate, PRG-2^{-/-} murine thalamic axons are not repelled, allowing them to enter LPA-rich zones. PRG proteins appear to function in an LPA-dependent manner as possible LPA-effectors, sensors, or scavengers in controlling axonal growth and navigation (Fink et al. 2017; Strauss and Bräuer 2013). There are several studies on PRG 1,3 and 5; however, there remains a dearth of information on PRG-2 and 4. A complete understanding of the functional mechanisms behind the lipid metabolism observed in PRGs could provide potential therapeutic strategies for neuropathological diseases. Based on these findings, I developed my thesis to investigate the role of PRG-2 and LPA-mediated signaling in the *Gallus gallus* visual system during neuronal development, using CRISPR-Cas9 receptor knockdown and GFP/PRG-2 plasmid overexpression.

Chapter Two
Materials and Methods

Determining PRG-2 Expression

To establish which PRG genes are expressed in the developing chicken eye, I used the *oneTaq* HotStart PCR kit. PCR was performed on RT+ and RT- samples compared to GAPDH for controls. To obtain RNA, 12 fertilized chicken eggs (provided by Tyson Foods) were incubated at 39°C until E6. Chicken embryos were then dissected, and their retinas were removed. E6 retinal RNA was obtained using the TRIzol™ Reagent isolation method. Two sets of primers for the chicken homologs of PRG-1,2,3,4, and 5 were designed using National Center for Biotechnology Information (NCBI's) Primer-BLAST tool (<http://www.ncbi.nlm.nih.gov/tools/primer-blast/>) (Table 1).

To quantify PRG-2 expression in the chicken retina and determine a developmental expression pattern, the retinas from E6, E7, E8, E10, and E12 chick embryos were dissected. RNA was isolated using the TRIzol™ Reagent isolation method. PCR was then performed on RT+ and RT- samples compared to GAPDH for controls.

Name	Sequence	Product Length
PRG3-1 Forward	GTCGCCTTGTTTCTGGGGATA	198
PRG3-1 Reverse	TGCTGCCAATCTTCCATCTCA	198
PRG3-2 Forward	GTGGAGGTGATTGAAAAGGCG	275
PRG3-2 Reverse	TGGACAACACATATCCCCAGAAA	275
PRG2-1 Forward	CGTAAGGTTTGTGGGTGTCC	267
PRG2-1 Reverse	GACACATAGACAGCGGCGAA	267
PRG2-2 Forward	ACTTCTTGGAGCTCACCGAC	193
PRG2-2 Reverse	AAGACGTGGACACCCACAAA	193
PRG1-1 Forward	TCTACTTCGTAGAGTTGCCAAT	269
PRG1-1 Reverse	GGCCTCTGTTCCAATCCCAT	269
PRG1-2 Forward	TTCTACTTCGTAGAGTTGCCAAT	272
PRG1-2 Reverse	TTGGCCTCTGTTCCAATCCC	272
PRG5-1 Forward	GGCCTCAGAGAGTGGTTGTG	187
PRG5-1 Reverse	GTGTCGCTTAGTTTCTGTCATTC	187
PRG5-2 Forward	TTCCCGCTGATGACCACTTC	261
PRG5-2 Reverse	GTGTCGCTTAGTTTCTGTCATTCA	261

Table 1: Primer sets for PRG-1,2,3,5 designed using NCBI Primer Blast. Each PRG had two sets of primers both the forward and reverse sequences are shown along with the associated product length.

gRNA Design

I designed six different gRNAs for *Gallus gallus* PRG-2 (aka PLPPR3) using the Benchling CRISPR gRNA design website (<https://www.benchling.com/crispr/>) (Table 2). From the gRNA sequences recommended by the Benchling website, I added my selected measures for the gRNAs based on a previous paper (Gandhi et al. 2017). First, I selected a sequence of 19 to 20 nucleotides in length adjacent to an NGG proto-spacer motif (PAM) sequence. Next, I ensured my gRNA would result in a cut between an exon and intron boundary. Oligonucleotides were ordered from Eurofin Genomics as forward and reverse primers and annealed to produce double-stranded oligos (Table 2). The annealed oligos were ligated into the U6.3>gRNA.fte vector (Gandhi et al. 2017; addgene: 99139) at the 5' and 3' overhangs. The U6.3>gRNA.fte vector was provided to our lab by Marianne Bronner.

PRG	Position	gRNA Sequence	PAM
PRG2-1	Exon-1	CAGGAGAGTCATGCTGTCCT	TGG
PRG2-2	Intron-2	TGCCCCCAGCTGCCCATCG	TGG
PRG2-3	Exon-3	GCGCCGCACCGTAAGGTTTG	TGG
PRG2-4	Exon-4	AGACAGGATGGCGTGCTTGT	CGG
PRG2-5	Exon-5	ACTCACCGACACATAGACAG	CGG
PRG2-6	Exon-2	CGCGCTCTCCATGCCCTACG	TGG

Table 2: Six different guide RNAs (gRNAs) for Gallus gallus PRG-2 (aka PLPPR3) were made using the Benchling CRISPR gRNA design website. Each sequence is a single-stranded DNA oligonucleotide with overhangs specifically designed to be used for ligation into the U6.3>gRNA.fte. vector targeting PRG-2. The associated PAM sequence and position dictates the general location of the cut that Cas9 will make and which intron or exon boundary the cut should be made.

The plasmid U6.3>gRNA.fte; addgene: 99139 was linearized with Bsal-HF with either 5'-GGAT-3' or 3'-CAAA-5' overhangs which allowed me to clone my annealed oligos into my vector. The ligation reaction was incubated for 20 minutes at room temperature (25-27°C). After incubation, high-efficiency 5-alpha Competent *E. coli* (DH5a; New England BioLabs) were transformed with the ligated gRNA vector. SOC Medium was used for the transformation procedure. *E. coli* cells were spread on pre-warmed LB agar plates containing 100 ug/ml carbenicillin. The ligation reaction produced over a hundred colonies in total.

gRNA Isolations

To screen for successful inserts, I isolated plasmid DNA using the Zymo research miniprep plasmid DNA purification kit. The transformed *E. coli* were left to grow in LB medium overnight. To determine if my gRNA ligated into the U6.3 vector, I PCR-amplified using U6 sequencing primers (5'-ATCGGCTAAGCGGGCCTAAG-3') with gRNA reverse primers. I confirmed that five of the gRNAs oligos were cloned into the U6.3>gRNA.fte vector through sequencing; gRNA6 was not successfully cloned. I stored my cloned gRNA vectors at -20°C.

Cell Culture, Transfection of DF1-Cas9 Cells

An immortalized chicken DF-1 fibroblast cell line expressing Cas9 (DF1-Cas9; Gandhi et al. 2017) was previously obtained. DF1-Cas9 cells were cultured at 37°C in 5% CO₂ in DMEM (Hyclone) supplemented with 10% fetal bovine serum (Gibco) and penicillin/streptomycin (Hyclone). To test gRNAs, DF1-Cas9 cells were transfected with each of the previously cloned gRNAs and tdTomato. DF1-Cas9 cells were seeded to achieve 80% confluency by the day of transfection. I used FuGene-HD reagent (Promega) for the transfections. The plasmid DNA was added to a mixture with the FuGene-HD reagent in a 3:1 ratio of FuGene-HD to plasmid DNA. I incubated my mixture for 10 minutes and added it to my DF-1/Cas9 cells. The cells grew for 2 days before analyzing my transfected cells under with fluorescence microscopy.

Cell Sorting, DNA Isolation

For analysis of transfected cell DNA via cell sorting, DF1-Cas9 cells were washed once with PBS and then harvested from their culture dish using Trypsin for 5 minutes at 37°C, then centrifugated for 5 minutes at 1500rpm. Cells were resuspended in phosphate-buffered saline (PBS) (Gibco) with 0.5% fetal bovine serum (FBS) and 0.1 mM EDTA at 400,000 cells/mL (according to Nanocollect WOLFsorter). The cells were then filtered (50 µm) to remove aggregates and then stored on ice. Cell sorting was done following the Nanocollect WOLFsorter manufacturer protocol. Each of the RNA/tdTomato transfected cells in 1.5 ml Eppendorf tubes were left on ice before DNA isolation.

Sorted cells were pelleted via centrifugation for 10 minutes at 3600 rpm, and the supernatant was removed. The pelleted tdTomato-positive cells were resuspended in a cell lysis solution (100 mM TrisCl, pH 8, 50 mM EDTA, 1% (w/v) sodium dodecyl

sulfate) until viscous. The cell lysate was centrifugated at max speed for 3 minutes using an Eppendorf tube, and the supernatant was transferred into a 1.5 ml Eppendorf tube containing 600 μ l of isopropanol, and mixed, followed by max centrifugation in an Eppendorf centrifuge for 1 minute at room temperature. The supernatant was removed, and the pellet was washed with 70% EtOH, followed by max centrifugation for 1 minute. The supernatant was removed, and the DNA pellet was air-dried. DNA was resuspended in nuclease-free H₂O and incubated overnight at room temperature to solubilize genomic DNA before PCR amplification.

PCR-amplification of Mutation

Primers were designed for Phusion High-Fidelity DNA Polymerase PCR using the PRG-2 genomic sequence found using NCBI's Primer-BLAST (<http://www.ncbi.nlm.nih.gov/tools/primer-blast/>). Using the following criteria: 1) the primers must have a T_m>55°C, 2) their length be between 18 and 22 base pairs, and 3) they had a 45 to 60% GC content. Table 3 shows the forward and reverse primer target locus and the expected amplicon of PCR production for each gRNA.

Name	Sequence	Product Length
PRG2-1 Forward	CATGATCTCCCCGAAGGAC	222
PRG2-1 Reverse	AGGGCTCAATGCCATCC	222
PRG2-3 Forward	CAGATCATGCTCGGGGAG	215
PRG2-3 Reverse	ACAGAGGGGTTCGGGTTC	215
PRG2-4/5 Forward	CCAACCCCTACATCACGC	285
PRG2-4/5 Reverse	GAGTTGAAGTACATCTGGAG	285
PRG2-7 Forward	TCTTCGCCTTCGCCATC	213
PRG2-7 Reverse	TGGTACGCCTGTGGGTA	213

Table 3: Design of forward and reverse primers for Phusion PCR-amplification over PRG 2-1,3,4,5,7 mutated genomic DNA regions of transfected DF-1 tdTomato-positive cells. Each primer should amplify the region mutated by the CRISPR system.

Mutation Validation

Transfected and sorted cell DNA was used for PCR amplification using Phusion High Fidelity with PRG-2 Phusion primers (Table 3). Amplicons were then gel purified (Zymo), and TA cloned into CloneJET PCR Cloning Kit (ThermoFisher) was transformed into high-efficiency 5-alpha Competent *E. coli* (DH5a; New England BioLabs) *E. coli* cells were spread on pre-warmed LB agar plates containing 50 µg/ml carbenicillin. The cloning reaction produced over a hundred colonies in total. Fifteen clones were selected for each gRNA, plasmid prep by miniprep, and sent off for sequencing at Eurofins Genomics. Sequences were compared using Clustal Omega Sequence alignment (<https://www.ebi.ac.uk/Tools/msa/clustalo/>).

Ex ovo Chicken Embryo Culture, Injection, and Electroporation Optimization

Fertilized chicken eggs were obtained from Tyson Farms. Eggs were incubated at 39°C with rocking and humidity for 2 days until experimental procedures. Solo plastic cups were weighted with 35 mL of sterilized distilled H₂O before a 4 cm-deep plastic hammock made of Saran brand plastic wrap was made and secured with a rubber band. Cup lids were given a single puncture for airflow, and the cups and lids were UV sterilized for 45 minutes. On embryonic day two (E2), embryos were *ex ovo* cultured in the plastic cups by cutting an opening to carefully transfer the entire contents of the eggs into *ex ovo* cups and placed into a 39°C incubator with water for humidity until E2. At E3, a 2:1 solution of water and 2627.5ng/ul tdTomato plasmid (addgene:30530), along with 0.05% Fast Green (for visualization), was injected into the subretinal space of the cupped embryo and electroporated using a BTX ECM 830 Electroporation Generator System that was set to 5 pulses of 15V for 50 ms with 950 ms intervals as previously described (Islam et al. 2012). Electroporated embryos were placed back in the incubator and allowed to develop until retinal dissections were done at E6.

Retinas were dissected by removing the iris to expose the retina from electroporated embryos on embryonic day 6 (Hamburger and Hamilton stages 28-29) under a fluorescence stereoscope. Dissected retinas were then imaged using a fluorescent microscope.

Overexpression of GFP-PRG-2 Construct

DF-1 cells were cultured at 37°C in 5% CO₂ in DMEM (Hyclone) supplemented with 10% fetal bovine serum (Gibco) and penicillin/streptomycin (Hyclone). DF-1 cells were transfected with either the GFP plasmid or my PRG2-Mouse in pcDNA3.1(+)-EGFP fusion protein plasmids. This plasmid was designed to express mouse PRG-2 and GFP fusion protein for visualization. DF-1 cells were seeded to achieve 80% confluency by the day of transfection. I used a lipid-based FuGene-HD reagent (Promega) for transfection. The DNA was added to a mixture with the FuGene-HD reagent in a 3:1 ratio of FuGene-HID to plasmid DNA. I incubated my mixture for 10 minutes and added it to my DF-1 cells. The next day I changed the media on the cells and allowed them to grow for 2 days before analyzing the transfected cells under confocal fluorescence microscopy.

Chapter 3

Results

Expression

PRGs are tightly regulated proteins expressed throughout different phases of brain development (Brauer 2008; Yu et al. 2015). Their differential expression suggests roles in neuronal development. Research on PRG has mainly focused on glutamatergic, hippocampal, and cortical neurons of mice, rats, and humans. However, their expression and localization patterns suggest roles in other brain regions and cell types (Fuchs et al. 2022). The primary goal of this research is to determine the function of PRG-2 in the neuronal development of the visual system and its interaction with LPA. To investigate this question, I first determined the expression of PRGs in the embryonic chicken eye using RT-PCR. Two sets of primers for the chicken homologs of PRG-1,2,3,4, and 5 were designed using National Center for Biotechnology Information (NCBI) Primer-BLAST tool (<http://www.ncbi.nlm.nih.gov/tools/primer-blast/>) (Table 1). PCR was performed on RT+ and RT- samples of the E6 retina using designed primers and compared to GAPDH as a control (Figure 2). I found that PRG-2,3 and 1 are expressed in the E6 chicken retina. PRG-5, however, was not expressed in the retina; but is expressed in the brain (data not shown). This suggested that PRGs possibly play a role in the retinal development of chickens. This also ensured that chickens are a good model organism to study PRG functions.

During Rat early developmental stages at embryonic (E) days E14-E16, PRG-3 mRNA was detected in the subventricular zone, ventricular zone, the cortical plate, and the hippocampal anlage (Savaskan et al. 2004; Wang and Molnár 2005). *In situ* hybridization and immunoblotting analyses identified PRG-2 expression from E14.5 onwards in thalamic and cortical brain regions (Cheng et al. 2016) with increasing mRNA and protein expression levels from E16 until early postnatal stages (Brosig et al. 2019). To quantify PRG-2 expression in the chicken retina and determine a developmental expression pattern, the retinas from E6, E7, E8, E10, and E12 chick embryos were

dissected, and RNA was isolated. PCR was then performed on RT+ and RT- samples. I found PRG-2 to be expressed throughout the development of the chicken retina, suggesting it has a potential role during similar developmental time periods for other organisms (Figure 3).

System to Mutate PRG-2 Using CRISPR

PRG-2 is essential for guiding thalamocortical axonal projections into the intermediate zone during development (Cheng et al. 2016). In this case, guidance depended on LPA and protein-protein interactions between PRG-2 and radixin. Interestingly, adult PRG-2 KO mice exhibited dampened neuronal activity at the cortical projection site and subsequent impaired local information processing shown by whisker-dependent sensory discrimination (Cheng et al. 2016). PRG proteins, specifically PRG-2, appear to function in an LPA-dependent manner as possible LPA-effectors, sensors, or scavengers in controlling axonal growth and navigation (Fink et al. 2017; Strauss and Bräuer 2013). Therefore, I hypothesized that RGC growth cones with a mutated PRG-2 will have reduced collapse when exposed to LPA at various concentrations. I designed 6 different gRNAs for *Gallus gallus* PRG-2 (aka PLPPR3) to test this hypothesis using the Benchling CRISPR gRNA design website (Table 2). I designed each gRNA to cut at an intron-exon boundary on the PRG-2 DNA sequence (Figure 4). After Cas9 made the cut and cell repair occurred, the resulting PRG-2 protein will hypothetically have noncoding (intronic) regions in the final product leading to loss of function.

CRISPR, however, is not 100% effective; for various reasons one gRNA could make a cut and induce a mutation 9 out of 10 times (90% mutation rate), and another could mutate 4 out of 10 or 40%. In order to pick the gRNA with the highest mutation rate, I first screened each of my gRNA by transfecting it along with tdTomato into DF-1 Cas9 cells. I then sorted the transfected cells to isolate the tdTomato-positive population. Afterward, I harvested the DNA of the tdTomato-positive cells and sent them for

sequence to identify the mutation rate. The gRNA cloning process for CRISPR resulted in a single gRNA with a 40% mutational rate and some others with no mutation (Table 4). To generate these mutation rates, 15 colonies from each transformation was collected and sent for sequencing. As stated before, a 40% mutation rate is too low to produce accurate results during experimentation. Despite the increasing specificity of CRISPR-Cas9 technology, some critical considerations still require comprehensive studies. Efforts to increase specificity have been conducted to improve RNA design (Gandhi et al. 2017)

To enhance the injection efficiency to deliver a CRISPR construct into the chick retina, I optimized the procedure. My *in vitro* data must have a statistically appropriate number of growth cones to analyze in order to compare mutated RGC growth cones against the control. I used the method of electroporation (i.e., an electric current is used to force the negatively charged DNA into the cells) to deliver the DNA after I had successfully microinjected plasmids into the subretinal space at E3 of development. To assess my co-electroporation efficiency, I then dissected the retina of the injected embryo on E6 and viewed them under a fluorescent microscope. The E6 embryo retina successfully took up my tdTomato injection solution (Figure 5). In order to achieve these results, I faced several obstacles that required optimization. The first being chicken viability which is naturally affected by age of the eggs before initial incubations as well as the cupping and injection procedure. Optimizations for both variables were done through multiple experiments.

System for Overexpression of PRG-2

Another way to determine the function of PRG-2 is by inducing its overexpression. Most studies have utilized overexpression or stable cell lines to study PRG localization in different cellular membrane systems (Fuchs et al. 2022). Interestingly, overexpression of different PRG family members enhances their plasma membrane

localization (Brosig et al. 2019; Yu et al. 2015). I hypothesized that RGC growth cones with overexpressed PRG-2/GFP construct would be more sensitive to LPA, and there would be increased collapse when exposed to lower concentrations. To test this hypothesis, I validated the overexpressed PRG-2 first in DF-1 cells to ensure the construct could be taken up. Using the PRG-2/GFP construct, I transfected these chicken fibroblast cells to confirm that my PRG-2/GFP fusion construct could be expressed and used confocal imaging to visualize the expression in the cells (Figure 6). After confirmation of my PRG-2/GFP construct expression, I proceeded to *ex ovo* cupping and injections. Unfortunately, injections and electroporation of PRG-2/GFP construct into the chicken retina depend on the embryo's viability after cupping and the injection procedure. For instance, initial incubations before cupping started with a sample size of 60 embryos and after cupping this sample size was reduced to 50. Injections likewise reduced this sample size to an average of 25. The number of surviving embryos further decreased to 10 during development from E3-E6, affected by such things as mold or irreparable damage from injections. Although this experiment was run multiple times because of viability issues, I did not collect growth cone collapse data.

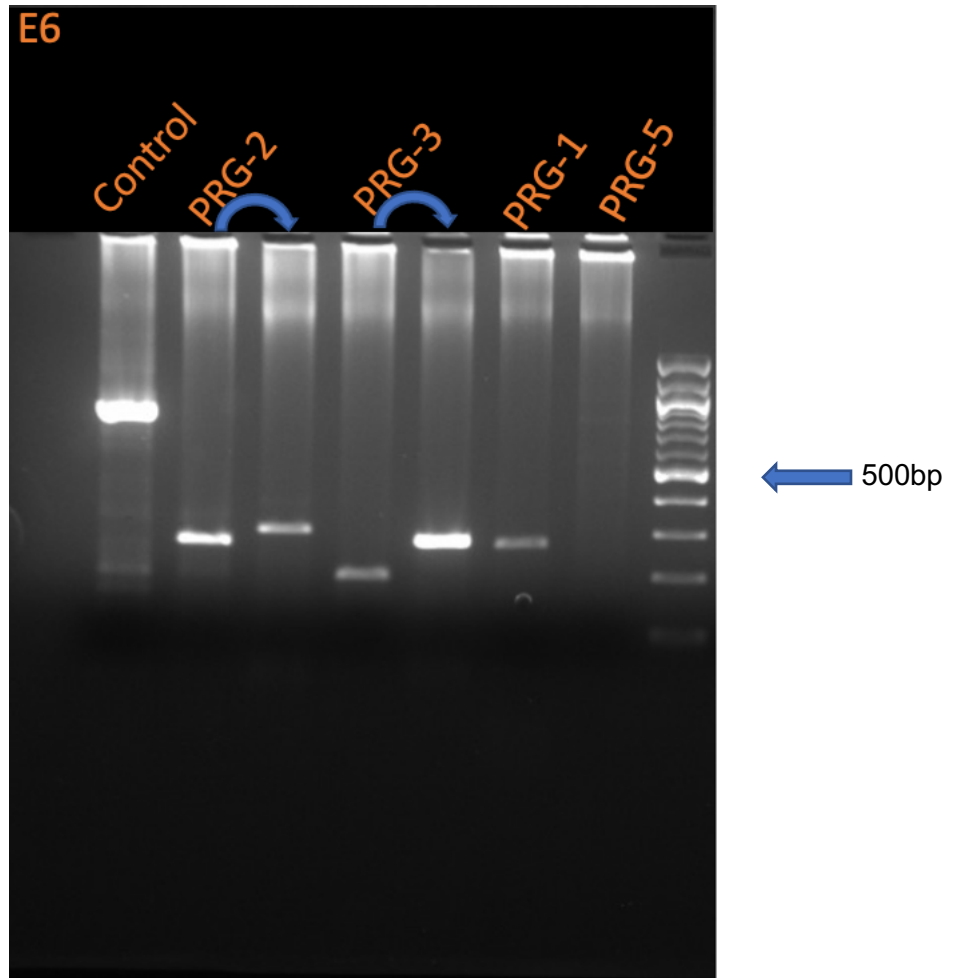


Figure 2: RT-PCR of E6 chicken retina using two sets of primers designed to detect PRG-2, and 3, mRNA and one set of primers for PRG-1, and 5. Bands seen in each lane left of the 100bp ladder correspond to the different PRGs. For a control, GAPDH (Control Lane) was used. A negative control without reverse transcriptase (RT) was also used (data not shown) and no bands were observed. Expected band sizes from left to right PRG-2: 272bp, 298bp, PRG-3:198bp, 275bp, PRG-1: 272bp, 269bp, PRG-5: 261bp.

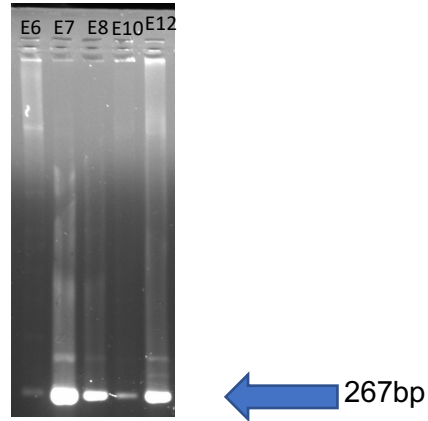


Figure 3: RT-PCR of the chicken retina from embryonic days E6, E7, E8, E10, E12 using PRG-2: 267bp specific primers and a 100bp ladder (not shown). PRG-2 is expressed throughout the chicken's development, as seen by the bands in each lane. For negative control, samples with no reverse transcriptase were used (data not shown).

Guide RNA Design (gRNA)

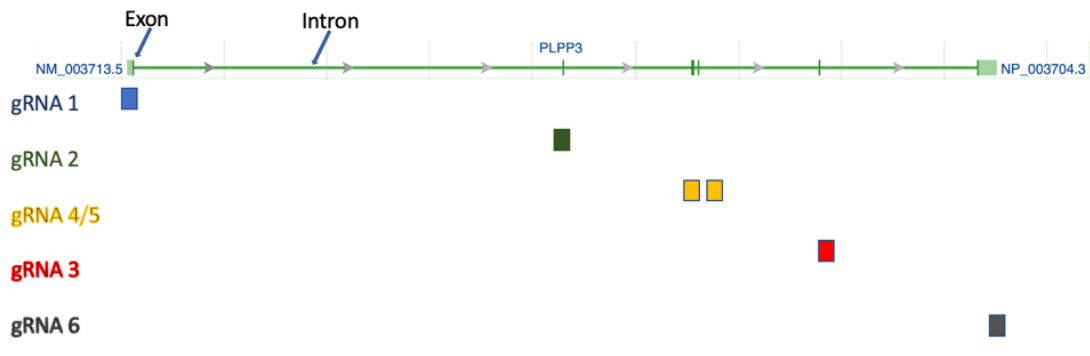


Figure 4: PRG-2 NCBI gene product map with Intron and Exon positions of designed gRNAs. PRG-2 (green line) has 6 Exons (green rectangles) and 5 introns (green space between the rectangles). The colored boxes show where each gRNA was designed to cut along the PRG-2 product.

Mutations In PRG-2 caused by gRNA 4 Sequences	
AGACAGGATGGCGTGCTTGT	Original
AGACAGGATGGCGTGCTT--	Mutation
AGACAGGATGGCGTGCTGT---	Mutation
AGACAGGATGGCGTGC-	Mutation
AGACAGGATGGCGTGCTTG-	Mutation
AGACAGGATGGCGTGCTTGT	No mutation
AGACAGGATGGCGTGCTTGT	No mutation
AGACAGGATGGCGTGCTTGT	No mutation
AGACAGGATGGCGTGCTTGT	No mutation
AGACAGGATGGCGTGCTTGT	No mutation
AGACAGGATGGCGTGCTTGT	No mutation
AGACAGGATGGCGTGCTTGT	No mutation
AGACAGGATGGCGTGCTTGT	No mutation
AGACAGGATGGCGTGCTTGT	No mutation
AGACAGGATGGCGTGCTTGT	No mutation
AGACAGGATGGCGTGCTTGT	No mutation
AGACAGGATGGCGTGCTTGT	No mutation

Mutations In PRG-2 caused by gRNA 1 Sequences	
CAGGAGAGTCATGCTGTCCT	Original
AGGACAGCATGACTCTCAT	No mutation
AGGACAGCATGACTCTCAT	No mutation
AGGACAGCATGACTCTCAT	No mutation
AGGACAGCATGACTCTCAT	No mutation
AGGACAGCATGACTCTCAT	No mutation
AGGACAGCATGACTCTCAT	No mutation
AGGACAGCATGACTCTCAT	No mutation
AGGACAGCATGACTCTCAT	No mutation
AGGACAGCATGACTCTCAT	No mutation
AGGACAGCATGACTCTCAT	No mutation
AGGACAGCATGACTCTCAT	No mutation
AGGACAGCATGACTCTCAT	No mutation
AGGACAGCATGACTCTCAT	No mutation

Mutations In PRG-2 caused by gRNA 3 Sequences	
GCGCCGCACCGTAAGGTTTG	Original
GCGCCGCACCGTAAGGTTTG	No Mutation
GCGCCGCACCGTAAGGTTTG	No Mutation
GCGCCGCACCGTAAGGTTTG	No Mutation
GCGCCGCACCGTAAGGTTTG	No Mutation
GCGCCGCACCGTAAGGTTTG	No Mutation
GCGCCGCACCGTAAGGTTTG	No Mutation
GCGCCGCACCGTAAGGTTTG	No Mutation
GCGCCGCACCGTAAGGTTTG	No Mutation
GCGCCGCACCGTAAGGTTTG	No Mutation
GCGCCGCACCGTAAGGTTTG	No Mutation
GCGCCGCACCGTAAGGTTTG	No Mutation
GCGCCGCACCGTAAGGTTTG	No Mutation
GCGCCGCACCGTAAGGTTTG	No Mutation

Table 4: Clones selected from gRNA 1,3,4, plasmid transformation, and sent for sequencing at Eurofins Genomics. The mutation rate that resulted from the CRISPR construct gRNA 4 had only 4 out of 10 of the samples mutated. The other gRNA shown (3 and 1) had no mutations.

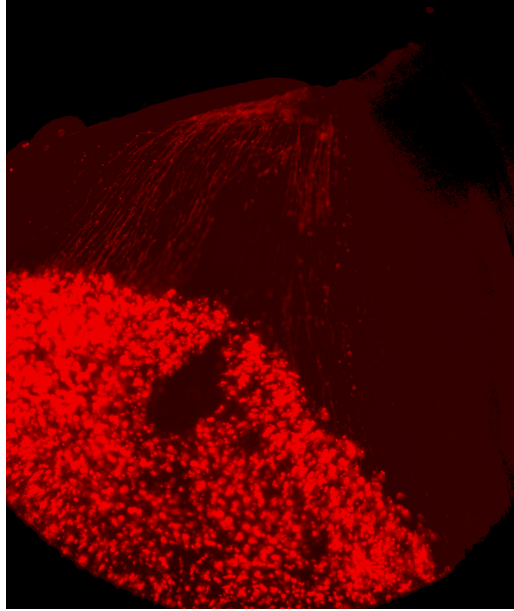


Figure 5: A fluorescent image of dissected E6 embryo retina that has successfully taken up my tdTomato injection solution from the optimization of ex ovo embryo cupping and injections. The dots are the labeled cell bodies and tracks are axons extending to form an optic nerve.

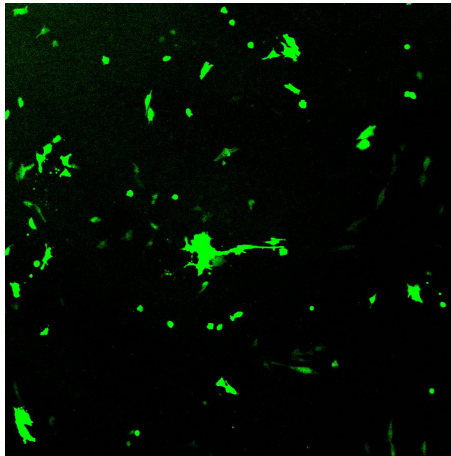


Figure 6: Using my PRG2-Mouse in pcDNA3.1(+)-EGFP fusion protein plasmids, DF-1 chicken fibroblast cells were transfected. To confirm that my GFP/PRG-2 fusion construct could be expressed transfected DF-1 cells (green shapes) were imaged using a confocal microscope.

Chapter Four

Discussion

System for Knockdown Of PRG-2 using CRISPR

PRG-2, like PRG-1, has a long 400 amino acid C-terminal domain. Additionally, PRG-2 has similar ectophosphatase domains to PRG-1 (Cheng et al. 2016). PRG-2 was shown to be involved with LPA-induced thalamic axonal guidance in mice, where LPA production was reduced by inhibiting autotaxin (an LPA synthesizing enzyme) which resulted in aberrant axonal extensions. Moreover, when grown on an LPA-rich substrate, PRG-2^{-/-} murine thalamic axons are not repelled, allowing them to enter LPA-rich zones. PRG proteins appear to function in an LPA-dependent manner as possible LPA-effectors, sensors, or scavengers in controlling axonal growth and navigation (Fink et al. 2017; Strauss and Bräuer 2013). To investigate whether or not LPA and PRG-2 play a similar role in RGC development, I hypothesized that RGC growth cones with a mutated PRG-2 will have reduced collapse when exposed to LPA at various concentrations. To test this, I designed six guide RNAs (gRNA) to PRG-2 for mutation with CRISPR-Cas9. I designed each gRNA to cut at an intron-exon boundary within the PRG-2 DNA sequence. I did this hoping that after Cas9 made the cut and cell repair occurred, the resulting PRG-2 protein would hypothetically have noncoding (intronic) regions in the final product leading to loss of function. However, the CRISPR-Cas9 system is not 100% effective. For instance, one gRNA could cut and induce a mutation only 4 out of 10 times or 40% and another at a higher rate. Because I co-electroporate with another plasmid, tdTomato, I could get explants that took up the tdTomato but do not have a mutation. In other words, neurites would look like they are generally behaving with no mutation even if they have taken up the florescent plasmid. However, following the design criteria did not result in mutations that could be used in this experiment. The gRNA cloning process for CRISPR resulted in a single gRNA with a 40% mutational rate and some with no mutations.

I have already determined the developmental expression of PRGs in the embryonic chicken eye using RT-PCR (Figure 2 and 3) and developed the tools to mutate PRG-2 in the developing chicken eye using CRISPR-Cas9 technology (Table 2). Using this data, a continuation of this project would first consist of optimizing the CRISPR constructs and revalidating their mutation rates. Using a validated construct to mutate the PRG-2 receptor and performing a growth cone collapse assay could produce a multitude of results. A typical growth cone collapse assay consists of dissected retinal ganglion cells explants being treated with media control or LPA at 1 μ M, 100nM, or 10nM concentrations, incubated for 10 minutes in a 37°C, 5% CO₂ incubator, then fixed. Growth cone collapse is quantified by counting isolated growth cones attached to neurites emanating from the explant using an inverted florescent microscope. They can then be categorized as collapsed or not and the percent collapsed can be calculated as previously done in our lab (Fincher et al. 2014). Figure 7 shows a typical growth cone collapse assay. However, RGC growth cones with a mutated PRG-2 may have reduced collapse when exposed to LPA, as I hypothesized (Figure 8). Alternatively, instead of seeing a attenuation for growth cone collapse, one could see a partial reduction in the number of growth cone collapses, suggesting PRG-2 modulates growth cone response to LPA but does not entirely control it (Figure 9). The neurite outgrowth activity of PRG likely involves LPA and other extracellular growth inhibition signals and associated receptors (Fuchs et al. 2022). In the extreme, we could see a complete attenuation of growth cone collapse (Figure 10).

System for Overexpression

Multiple studies have suggested that PRG 1,4, and 5 following overexpression in neuronal cell lines result in aberrant LPA downstream signaling and its effects on cellular morphology and neurite retraction (Agbaegbu Iweka et al. 2021; Bräuer et al. 2003; Brogгинi et al. 2016). The proposed mechanisms for these aberrant signals involve the

engagement of RhoA in inactive complexes with RhoGDI following the overexpression of PRG-1. Similarly, overexpression of PRG-5 reduces LPA-activated RhoA in cell lines. Thus, a pattern emerges that PRGs may function as a fine-tuning device for LPA-induced RhoA activity and its biological effects (Fuchs 2022). For these reasons, I hypothesized that RGC growth cones with overexpressed PRG-2/GFP construct would be more sensitive to LPA. If exposed to this axon guidance molecule during an assay, there would be increased growth cone collapse at lower concentrations (Figure 11).

To test this hypothesis, I had to establish the overexpression of PRG-2 first in DF-1 cells to ensure the construct could be taken up and expressed. Using the PRG-2/GFP construct, I transfected chicken fibroblast cells and confirmed overexpression by confocal imaging. This established that my mouse construct could be expressed in chickens. After confirming the expression by confocal imaging, I proceeded to retinal injections. Unfortunately, injections and electroporation of the PRG-2/GFP construct into the chicken retina depend on the embryo's viability after cupping and the injection procedure. *Ex ovo* cupping exposes the developing embryo to a host of variables that often result in the death of the developing embryo. Compounding this is the natural chicken viability. Not all embryos will develop to the stages needed to perform experiments. Because of viability issues, I did not collect growth cone collapse data. Further data in the form of western blotting would also be needed to ensure the entire fusion protein is being expressed and not just GFP. Although this has been partially done through the confocal imaging; cells sometimes process protein-protein constructs in different ways. For instance, the PRG-2 part of the construct could be cleaved off during protein processing resulting in expression of only GFP and not PRG-2. After confirmation, injections and electroporation could be performed to interrogate the functions of PRG-2.

Overall, there are still some important considerations when investigating PRG-2 that require comprehensive studies; currently we lack the molecular insight needed to understand the functional implications of the PRG and LPA signaling interactions during development. Ongoing studies of PRG KO mice and PRG polymorphisms in humans suggest a dominant role of PRG deficiency for several CNS diseases. Moreover, there are several lines of evidence suggesting PRGs may affect the regeneration processes following CNS injury (Fuchs et al. 2022). Elucidating the roles of PRGs in CNS disease could result in the emergence of PRG as a novel pharmacological target.

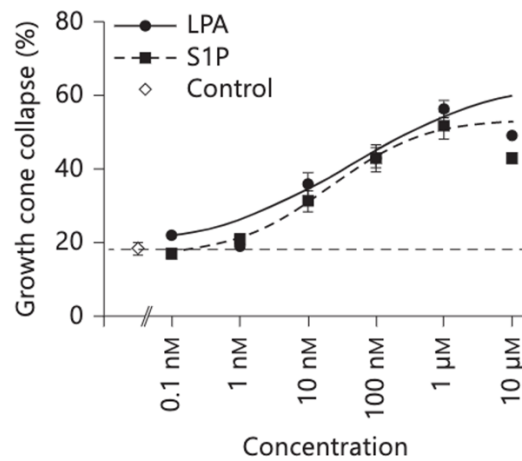


Figure 7: A typical growth cone collapse response to LPA is shown by the solid black line and S1P (another guidance cue) by the dashed line. At the lower concentration, there is minor collapse but as the concentration increases, so does the growth cone collapse (Fincher et al. 2014).

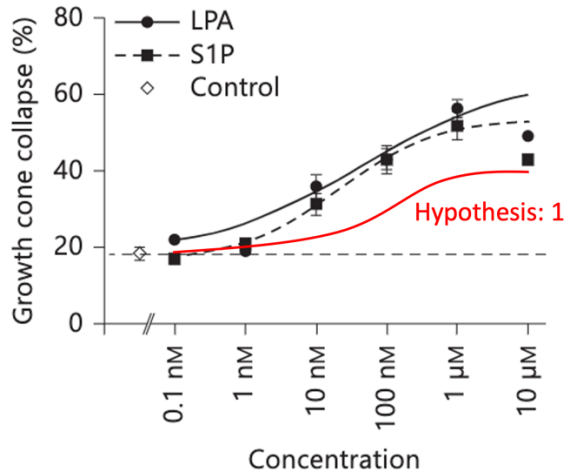


Figure 8: For my first hypothesis, if PRG-2 interacted with LPA normally resulting in a collapse response, when PRG-2 is mutated, I expect the growth cone collapse to be less, even in the higher LPA concentrations (red line).

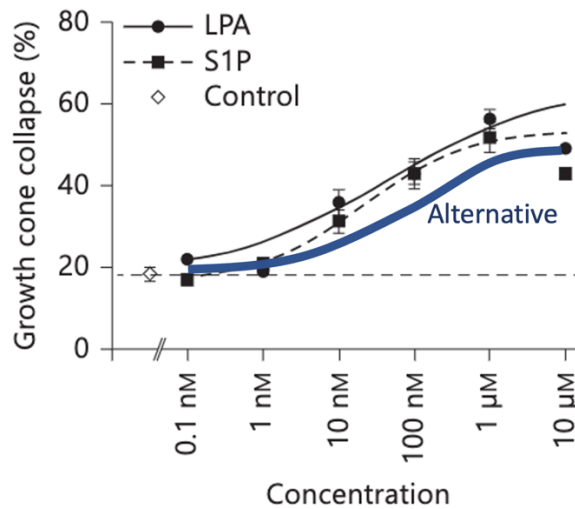


Figure 9: For my alternative hypothesis, if PRG-2 was not the only receptor that modulates response to LPA, I would expect that instead of seeing a complete attenuation for growth cone collapse, one could see a partial reduction in the number of growth cone collapses, suggesting PRG-2 modulates growth cone response to LPA but does not entirely control them (bold blue line).

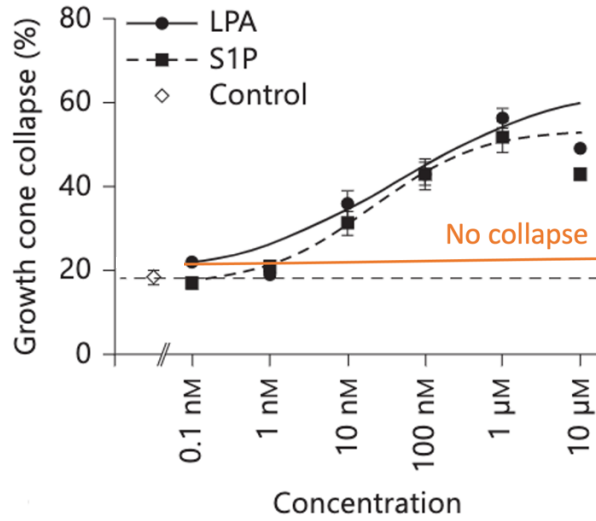


Figure 10: The orange line is an extreme case in which I hypothesized that mutation of PRG-2 through CRISPR could result in a complete attenuation of growth cone collapse.

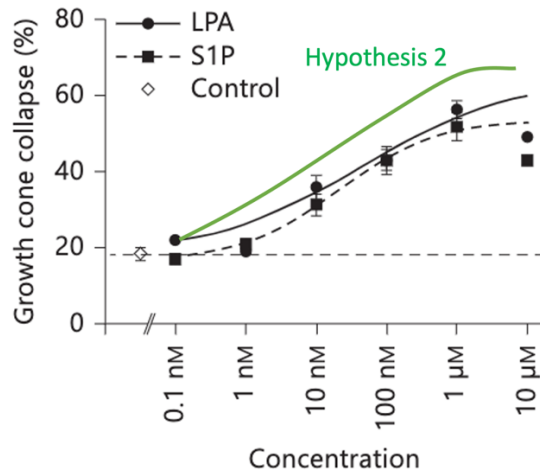


Figure 11: If PRG-2 was overexpressed in RGCs then the LPA response would increase. Thus, I hypothesized that RGC growth cones with overexpressed PRG-2/GFP construct would be more sensitive to LPA (green line). If exposed to this axon guidance molecule during an assay, there would be increased growth collapse at lower concentrations.

References

- Agbaegbu Iweka C, Hussein RK, Yu P, Katagiri Y, Geller HM. 2021. The lipid phosphatase-like protein plppr1 associates with rhogdi1 to modulate rhoa activation in response to axon growth inhibitory molecules. *J Neurochem.* 157(3):494-507.
- Alderton F, Darroch P, Sambhi B, McKie A, Ahmed IS, Pyne N, Pyne S. 2001. G-protein-coupled receptor stimulation of the p42/p44 mitogen-activated protein kinase pathway is attenuated by lipid phosphate phosphatases 1, 1a, and 2 in human embryonic kidney 293 cells. *J Biol Chem.* 276(16):13452-13460.
- Birgbauer E. 2021. Lysophosphatidic acid signalling in nervous system development and function. *Neuromolecular Med.* 23(1):68-85.
- Birgbauer E, Chun J. 2010. Lysophospholipid receptors lpa(1-3) are not required for the inhibitory effects of lpa on mouse retinal growth cones. *Eye and brain.* 2:1-13.
- Brauer AR, N. 2008. Plasticity-related genes (prgs/lrps): A brain-specific class of lysophospholipid-modifying proteins. *Biochim Biophys Acta.* 1781(9):595-600.
- Bräuer AU, Savaskan NE, Kühn H, Prehn S, Ninnemann O, Nitsch R. 2003. A new phospholipid phosphatase, prg-1, is involved in axon growth and regenerative sprouting. *Nat Neurosci.* 6(6):572-578.
- Broggini T, Nitsch R, Savaskan NE. 2010. Plasticity-related gene 5 (prg5) induces filopodia and neurite growth and impedes lysophosphatidic acid- and nogo-a-mediated axonal retraction. *Mol Biol Cell.* 21(4):521-537.
- Broggini T, Schnell L, Ghoochani A, Mateos JM, Buchfelder M, Wiendieck K, Schäfer MK, Eyupoglu IY, Savaskan NE. 2016. Plasticity related gene 3 (prg3) overcomes myelin-associated growth inhibition and promotes functional recovery after spinal cord injury. *Aging.* 8(10):2463-2487.
- Brosig A, Fuchs J, Ipek F, Kroon C, Schrötter S, Vadhvani M, Polyzou A, Ledderose J, van Diepen M, Holzhütter H-G et al. 2019. The axonal membrane protein prg2 inhibits pten and directs growth to branches. *Cell Rep.* 29(7):2028-2040.e2028.
- Cheng J, Sahani S, Hausrat Torben J, Yang J-W, Ji H, Schmarowski N, Endle H, Liu X, Li Y, Böttche R et al. 2016. Precise somatotopic thalamocortical axon guidance depends on lpa-mediated prg-2/radixin signaling. *Neuron.* 92(1):126-142.
- Coiro P, Stoenica L, Strauss U, Bräuer AU. 2014. Plasticity-related gene 5 promotes spine formation in murine hippocampal neurons *. *J Biol Chem.* 289(36):24956-24970.
- Erskine L, Herrera E. 2007. The retinal ganglion cell axon's journey: Insights into molecular mechanisms of axon guidance. *Dev Biol.* 308(1):1-14.
- Fincher J, Whiteneck C, Birgbauer E. 2014. G-protein-coupled receptor cell signaling pathways mediating embryonic chick retinal growth cone collapse induced by lysophosphatidic acid and sphingosine-1-phosphate. *Dev Neurosci.* 36(6):443-453.
- Fink KL, López-Giráldez F, Kim I-J, Strittmatter SM, Cafferty WBJ. 2017. Identification of intrinsic axon growth modulators for intact cns neurons after injury. *Cell Rep.* 18(11):2687-2701.
- Fuchs J, Bareesel S, Kroon C, Polyzou A, Eickholt BJ, Leondaritis G. 2022. Plasma membrane phospholipid phosphatase-related proteins as pleiotropic regulators of neuron growth and excitability. *Front Mol Neurosci.* 15:984655.
- Fukushima N, Ishii I, Contos JJA, Weiner JA, Chun J. 2001. Lysophospholipid receptors. *Annual Review of Pharmacology and Toxicology.* 41(1):507-534.
- Huberman AD, Wang G-Y, Liets LC, Collins OA, Chapman B, Chalupa LM. 2003. Eye-specific retinogeniculate segregation independent of normal neuronal activity. *Science (New York, NY).* 300(5621):994-998.
- Huebner EA, Strittmatter SM. 2009. Axon regeneration in the peripheral and central nervous systems. In: Koenig E, editor. *Cell biology of the axon.* Berlin, Heidelberg: Springer Berlin Heidelberg. p. 305-360.
- Liu X, Huai J, Endle H, Schlüter L, Fan W, Li Y, Richers S, Yurugi H, Rajalingam K, Ji H et al. 2016. Prg-1 regulates synaptic plasticity via intracellular pp2a/β1-integrin signaling. *Dev Cell.* 38(3):275-290.
- Mietto BS, Mostacada K, Martinez AMB. 2015. Neurotrauma and inflammation: Cns and pns responses. *Mediators Inflamm.* 2015:251204.

- Richardson PM, McGuinness UM, Aguayo AJ. 1980. Axons from CNS neurons regenerate into PNS grafts. *Nature*. 284(5753):264-265.
- Savaskan NE, Bräuer AU, Nitsch R. 2004. Molecular cloning and expression regulation of prg-3, a new member of the plasticity-related gene family. *Eur J Neurosci*. 19(1):212-220.
- Schneider P, Petzold S, Sommer A, Nitsch R, Schwegler H, Vogt J, Roskoden T. 2018. Altered synaptic phospholipid signaling in prg-1 deficient mice induces exploratory behavior and motor hyperactivity resembling psychiatric disorders. *Behav Brain Res*. 336:1-7.
- Schwab M, Caroni P. 1988. Oligodendrocytes and CNS myelin are nonpermissive substrates for neurite growth and fibroblast spreading in vitro. *The Journal of Neuroscience*. 8(7):2381-2393.
- Strauss U, Bräuer AU. 2013. Current views on regulation and function of plasticity-related genes (prgs/lprs) in the brain. *Biochim Biophys Acta*. 1831(1):133-138.
- Tessier-Lavigne M, Goodman CS. 1996. The molecular biology of axon guidance. *Science*. 274(5290):1123-1133.
- Tokumitsu H, Hatano N, Tsuchiya M, Yurimoto S, Fujimoto T, Ohara N, Kobayashi R, Sakagami H. 2010. Identification and characterization of prg-1 as a neuronal calmodulin-binding protein. *Biochem J*. 431(1):81-91.
- Trimbuch T, Beed P, Vogt J, Schuchmann S, Maier N, Kintscher M, Breustedt J, Schuelke M, Streu N, Kieselmann O et al. 2009. Synaptic prg-1 modulates excitatory transmission via lipid phosphate-mediated signaling. *Cell*. 138(6):1222-1235.
- Velmans T, Battfeld A, Geist B, Farrés AS, Strauss U, Bräuer AU. 2013. Plasticity-related gene 3 promotes neurite shaft protrusion. *BMC Neurosci*. 14(1):36.
- Vogt NM, Kerby RL, Dill-Mcfarland KA, Harding SJ, Merluzzi AP, Johnson SC, Carlsson CM, Asthana S, Zetterberg H, Blennow K et al. 2017. Gut microbiome alterations in Alzheimer's disease. *Sci Rep*. 7(1).
- Wang W-Z, Molnár Z. 2005. Dynamic pattern of mRNA expression of plasticity-related gene-3 (prg-3) in the mouse cerebral cortex during development. *Brain Res Bull*. 66(4-6):454-460.
- Waxenbaum JA, Reddy V, Varacallo M. 2021. *Anatomy, autonomic nervous system*. StatPearls Publishing, Treasure Island (FL).
- Yu P, Agbaegbu C, Malide DA, Wu X, Katagiri Y, Hammer JA, Geller HM. 2015. Cooperative interactions of lpr family members in membrane localization and alteration of cellular morphology. *J Cell Sci*. 128(17):3210-3222.